Optimal dynamic stabilisation of a linear system by periodic stiffness excitation

Fadi Dohnal

Institute of Sound and Vibration Research, University of Southampton, Highfield SO17 1BJ, UK

Abstract

A theoretical study on the dynamic stabilisation of an unstable mechanical structure is performed. The system is unstable due to negative damping introduced by, for example, a self-excitation of linearised van der Pol type. A minimum model possessing two degrees of freedom with linear spring and damper elements is considered. Based on the effect of a parametric anti-resonance such a system may be stabilised by introducing a time-periodic stiffness variation. Optimum conditions are derived for achieving damping by parametric excitation. All stiffness elements in the system are considered to be available for stiffness variation. Using the averaging method in combination with Fourier series, general conditions for full vibration suppression are derived for arbitrary locations and phase relations of the stiffness variations. Analytical conditions are presented, showing how the maximum gain in stability depends on the amplitude, the phase, the location and the shape function of the periodic stiffness excitation. It is shown that only four characteristic values determine the optimum stiffness variation. These analytical predictions are verified by a numerical stability analysis of an example system. The results can be applied to tune the efficiency of vibration suppression achieved by a periodic variation of one or more stiffness parameters.
© 2008 Elsevier Ltd. All rights reserved.

1. Introduction

Parametrically excited vibrations represent a dangerous phenomenon in many engineering fields, such as the vibrations of rotating machinery [1], the roll motion of ships [2], the vibration of gears [3] or the dynamic stability of elastic structures [4]. A parametric excitation occurs if a physical parameter in the system is varied periodically in time leading to rheonomic equations of motion. In general, a parametric excitation introduces parametric resonances that may destabilise the system's vibration at double or combinational values of the natural frequencies introducing so-called parametric resonances or parametric instabilities. This effect is widely examined, see e.g. Refs. [4–12] and the literature cited therein for an overview over the most commonly used methods to analyse rheonomic systems. A parametric resonance is more dangerous than an ordinary resonance as it is characterized by exponential growth of the response amplitudes even in the presence of damping [12]. Investigations so far were focused on those cases, where parametric resonances appeared to be

---

E-mail address: fd@isvr.soton.ac.uk

resonant. However, during the last decade an interesting phenomenon has been discovered [13] that a non-resonant parametric resonance may occur if the system's parameters are tuned accordingly.

The main objective of this paper is to investigate the phenomenon that partial or even full vibration suppression of an unstable system can be achieved by interaction with parametric excitation. The system under consideration is dynamically unstable due to negative damping as commonly observed in the context of self-excited vibrations, for example, vibrations induced by dry friction [14] or by steady wind flow [15]. It is well known that the vibrations in negatively damped systems can be suppressed by using different kinds of passively damped spring-mass absorbers, see e.g. Ref. [16]. An interesting semi-active vibration suppression mechanism is the deliberate interaction with parametric excitation. This idea was first proposed in monograph [13], where conditions for full vibration suppression have been formulated mathematically based on Ref. [17] and later, using another approach, in Refs. [18–20]. It was found that the vibrations of a negatively damped system can be fully cancelled by parametric excitation within a frequency interval near a parametric combination resonance frequency of n-th order of the summation- or difference-type

$$\eta_0^{(n)} = \frac{|\Omega_1 \mp \Omega_2|}{n}, \qquad n = 1, 2, \ldots \tag{1}$$

Herein, frequencies Ω_1 and Ω_2 are the natural frequencies of the system and η_0 is the frequency of the parametric excitation. If a vibration suppression occurs at the parametric resonance frequency it is called parametric *anti*-resonance frequency [21].

In these preliminary works mainly the special case of a time-harmonic stiffness variation of a single stiffness coefficient has been investigated to achieve vibration suppression of an unstable two-mass system. A first step towards non-harmonic stiffness functions was investigated numerically in Ref. [22] and analytically in Ref. [23], where a rectangular stiffness variation is proposed. The variation of more than one stiffness coefficient, a multi-location parametric stiffness excitation, was examined for systems with special symmetry in Refs. [19,24,25] and for the most general linear system with two degrees of freedom and arbitrary phase relations between stiffness excitations can be found in Refs. [26,27].

The current contribution investigates conditions for an optimal configuration of a multi-location parametric stiffness excitation by employing the analytical results found in Ref. [27] resulting from the averaging method of first order as presented in Refs. [19,28]. In the following paragraphs, analytical conditions for vibration suppression are given that enable to determine the optimal non-harmonic shape, location and phase relations of multiple parametric stiffness excitations. The following analysis will show the interesting result that only four parameters are needed to determine the optimal shape, location and phase of a parametric stiffness excitation that maximises the parametric anti-resonance. It should be highlighted that the optimisation performed is restricted to systems for which the stability boundary curves can be approximated adequately by a first-order perturbation. Further study is needed if the contribution of a second-order perturbation cannot be neglected, as for the system in Refs. [18,29].

2. Problem definition

The most general linear two-mass system is analysed possessing linear stiffness and damping coefficients. The system is shown in Fig. 1 and may represent two modes of a vibrating structure. For an originally nonlinear system, the coefficients represents linearised expressions around the system's trivial equilibrium. Any of the stiffness coefficients is varied periodically with the same frequency η and the same periodic shape function $g(\eta t)$ but with different relative phase angles α_{12} and α_{02},

$$k_{01}(t) = k_{01}(1 + \varepsilon_{01} g(\eta t)),$$

$$k_{12}(t) = k_{12}(1 + \varepsilon_{12} g(\eta t + \alpha_{12})),$$

$$k_{02}(t) = k_{02}(1 + \varepsilon_{02} g(\eta t + \alpha_{02})). \tag{2}$$

The variation of the stiffness coefficient $k_{01}(t)$ is chosen to be the reference variation. Variables ε_{kl} are amplitude amplification factors of the corresponding stiffness parameters k_{kl} with $|\varepsilon_{kl}| < 1$. The equations of
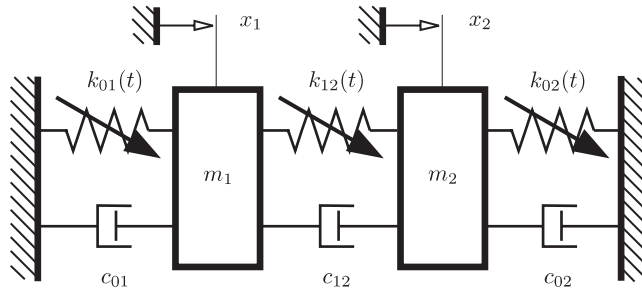
Fig. 1. Mechanical system with multi-location parametric stiffness variation.
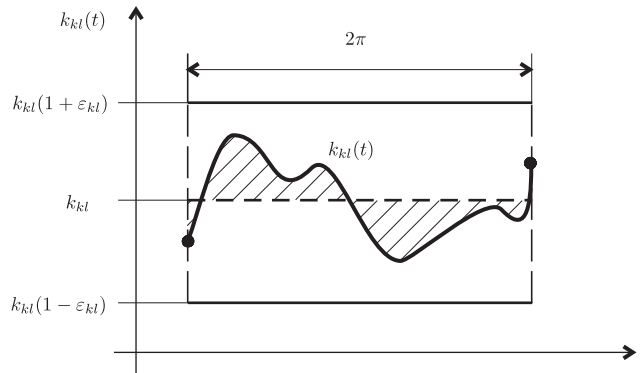

Fig. 2. General time-periodic stiffness variation.

motion can be written as

$$\mathbf{M}\ddot{\mathbf{x}}(t) + \mathbf{C}\dot{\mathbf{x}}(t) + \mathbf{K}(t)\mathbf{x}(t) = \mathbf{0}, \tag{3}$$

with the symmetric system matrices

$$\mathbf{M} = \begin{bmatrix} m_1 & 0 \\ 0 & m_2 \end{bmatrix}, \quad \mathbf{C} = \begin{bmatrix} c_{01} + c_{12} & -c_{12} \\ -c_{12} & c_{12} + c_{02} \end{bmatrix}, \quad \mathbf{K}(t) = \begin{bmatrix} k_{01}(t) + k_{12}(t) & -k_{12}(t) \\ -k_{12}(t) & k_{12}(t) + k_{02}(t) \end{bmatrix}.$$

Searching for an optimal shape function $g(\eta t)$ for the stiffness variations $k_{kl}(t)$ that can be regular functions or functions with a finite number of finite discontinuities in the interval $[0, 2\pi]$. Additionally, the following side conditions shall apply, as sketched in Fig. 2:

(i) The variation is periodic $g(0) = g(2\pi/\eta)$,
(ii) has a zero mean value and,
(iii) is bounded in between a stiffness bandwidth which is defined as

$$k_{kl}(1 - \varepsilon_{kl}) \leqslant k_{kl}(t) \leqslant k_{kl}(1 + \varepsilon_{kl}). \tag{4}$$

The first condition is proposed since the quenching effect is only known for periodic variations. The second side condition guarantees that the mean value of each stiffness excitation $k_{kl}(t)$ remains unchanged under $g(\eta t)$ in Eq. (2) to avoid shifts in the natural frequencies Ω_1, Ω_2. The last side condition is a physical requirement to avoid solutions that result in unbounded stiffness amplitudes. All physically reasonable signals meet these Dirichlet Fourier series conditions and, consequently, possess a Fourier series associated to its function representation. Without loss of generality the following study is restricted to Fourier cosine series of the form

$$g(\eta t) = \sum_{n=1}^{\infty} a_n \cos n\eta t, \quad a_n = \frac{1}{\pi} \int_0^{2\pi} g(t) \cos(nt)\, \mathrm{d}t. \tag{5}$$

By introducing the Fourier series in Eq. (5) the stiffness variations in Eq. (2) become

$$k_{kl}(t) = k_{kl}(1 + \varepsilon_{kl}g(\eta t + \alpha_{kl})) = k_{kl} + \varepsilon_{kl}k_{kl}\sum_{n=1}^{\infty} a_n(\cos \alpha_{kl}\cos(n\eta t) - \sin \alpha_{kl}\sin(n\eta t)), \quad (6)$$

with $kl = 01, 12, 02$ and $\alpha_{01} = 0$. Hence, the time-periodic stiffness matrix can be split into a constant part, the mean value, and two harmonic parts

$$\mathbf{K}(t) = \mathbf{K}_0 + \sum_{n=1}^{\infty} a_n(\mathbf{K}_c \cos(n\eta t) + \mathbf{K}_s \sin(n\eta t)). \quad (7)$$

A transformation matrix $\mathbf{T}$ is introduced

$$\mathbf{T} = \begin{bmatrix} 1 & 1 \\ t_1 & t_2 \end{bmatrix}, \qquad t_1 = 1 + \frac{k_{01} - m_1\Omega_1^2}{k_{12}}, \qquad t_2 = 1 + \frac{k_{01} - m_1\Omega_2^2}{k_{12}}, \quad (8)$$

where Ω_1 and Ω_2 are the system's undamped natural frequencies. By applying this transformation the mean value matrix $\mathbf{M}^{-1}\mathbf{K}_0$ becomes diagonal,

$$\mathbf{T}^{-1}\mathbf{M}^{-1}\mathbf{K}_0\mathbf{T} = \mathbf{\Omega}^2, \quad \varepsilon\mathbf{\Theta} = \mathbf{T}^{-1}\mathbf{M}^{-1}\mathbf{C}\mathbf{T}, \quad \varepsilon\mathbf{Q} = \mathbf{T}^{-1}\mathbf{M}^{-1}\mathbf{K}_c\mathbf{T}, \quad \varepsilon\mathbf{P} = \mathbf{T}^{-1}\mathbf{M}^{-1}\mathbf{K}_s\mathbf{T}, \quad (9)$$

with a scaling factor ε and

$$\mathbf{\Omega} = \begin{bmatrix} \Omega_1 & 0 \\ 0 & \Omega_2 \end{bmatrix}, \quad \mathbf{\Theta} = \begin{bmatrix} \Theta_{11} & \Theta_{12} \\ \Theta_{21} & \Theta_{22} \end{bmatrix}, \quad \mathbf{Q} = \begin{bmatrix} Q_{11} & Q_{12} \\ Q_{21} & Q_{22} \end{bmatrix}, \quad \mathbf{P} = \begin{bmatrix} P_{11} & P_{12} \\ P_{21} & P_{22} \end{bmatrix}. \quad (10)$$

The system is transformed into the modal space of the time-independent system at $\varepsilon_{kl} = 0$, its quasi-normal form

$$\ddot{\mathbf{y}}(t) + \varepsilon\mathbf{\Theta}\dot{\mathbf{y}}(t) + \mathbf{\Omega}^2\mathbf{y}(t) = -\varepsilon\sum_{n=1}^{\infty} a_n(\mathbf{Q}\cos(n\eta t) + \mathbf{P}\sin(n\eta t))\mathbf{y}(t). \quad (11)$$

3. Stability analysis

Closed form solutions of rheonomic differential equations as in Eq. (11) are only known for a few special cases. Approximate methods are good instruments for gaining deeper insight into mechanical systems where negative damping and time-periodic coefficients coexist. Among several perturbation methods [30,28], the application of the averaging method as proposed in Refs. [18,19] has turned out to be straight-forward for problems as investigated here. From now on the scaling factor ε in Eq. (11) is assumed to be sufficiently small to allow a first-order approximation.

In case of a variation of a single stiffness element only or a synchronous variation of multiple stiffness elements ($\alpha_{12} = 0 = \alpha_{02}$), the condition $\mathbf{P}_n = \mathbf{0}$ holds for the coefficient matrices in Eq. (11). The stability of such systems is discussed analytically in great detail in Refs. [13,18–20] applying different perturbation techniques. Introducing phase shifts between single stiffness excitations ($\alpha_{12}, \alpha_{02} \neq 0$) corresponds to a general harmonic stiffness variation for which $\mathbf{P}_n \neq \mathbf{0}$ in Eq. (11). An analytical stability analysis of this generalised system can be found in Refs. [26,27] which leads to cumbersome expressions. However, for a system with a diagonal inertia matrix $\mathbf{M}$ as introduced in Eq. (3), the matrix coefficients obey the relation

$$Q_{12}P_{21} - P_{12}Q_{21} = 0 \quad (12)$$

in which case the stability conditions are similar to the conditions derived for an excitation of a single stiffness element only.

For a first-order approximation, a small detuning from the parametric excitation frequency η_0 in Eq. (1) of the following form is introduced

$$\eta = \eta_0^{(n)} + \varepsilon\sigma^{(n)}. \quad (13)$$

Averaging at different frequencies η_0 and applying the Routh–Hurwitz criteria for complex polynomials in Refs. [31,32] leads to the following summarised stability conditions for Eq. (11) (more details can be found in Ref. [27] respecting Eq. (12)):

(i) In general, if the stiffness variation frequency η is not close to any of the frequencies in Eq. (1) or the parametric resonance frequencies $2\Omega_1/n$ or $2\Omega_2/n$, then the system is stable if and only if

$$\Theta_{11} > 0 \qquad \text{and} \qquad \Theta_{22} > 0. \tag{14}$$

If these conditions hold there is no negative modal damping present in the system and, hence, the system is stable.

(ii) If both conditions in Eq. (14) are not fulfilled then damping by interaction with parametric excitation is not possible.

(iii) If one of the condition in Eq. (14) is not satisfied then the system is unstable but may be stabilised if the stiffness variation frequency η is chosen to be close to a parametric anti-resonance frequency in Eq. (1). In this special case the stability conditions in Eq. (1) are no longer valid and are modified to the following new set of stability conditions. For the case of $\sigma = 0$ in Eq. (13), the stiffness variation frequency matches the parametric anti-resonance frequency exactly, $\eta = \eta_0^{(n)}$, and the stability conditions are

$$\Theta_{11} + \Theta_{22} > 0, \qquad \Delta^{(n)} = \Theta_{11}\Theta_{22} \pm a_n^2 \frac{Q_{12}Q_{21} + P_{12}P_{21}}{4\Omega_1\Omega_2} > 0. \tag{15}$$

For the case of $\sigma \neq 0$ in Eq. (13), the following conditions hold:

$$\Theta_{11} + \Theta_{22} > 0, \qquad \frac{|\Omega_1 \mp \Omega_2|}{n} - \varepsilon\sigma^{(n)} < \eta < \frac{|\Omega_1 \mp \Omega_2|}{n} + \varepsilon\sigma^{(n)}, \tag{16}$$

with the stability width

$$2\varepsilon\sigma^{(n)} = \frac{\Theta_{11} + \Theta_{22}}{n} \sqrt{-\frac{\Delta^{(n)}}{\Theta_{11}\Theta_{22}}}, \tag{17}$$

in analogy to Ref. [27]. Eq. (16) determines the boundary between stable and unstable system parameter values according to Eq. (13). The additional condition in Eq. (15) is needed to decide which side of the boundary is stable and which is unstable. Note that the stability conditions Eqs. (15), (16) are equivalent to the conditions derived in Refs. [13,19,21] for the case of $n = 1$, $a_i = 0$, $b_i = 0$, $\alpha_{kl} = 0$ but $a_1 = 1$. If the second condition in Eq. (15) is fulfilled for a certain value of n then the frequency $\eta_0^{(n)}$ is called a parametric *anti*-resonance frequency. The frequency interval of this anti-resonance is $2\varepsilon\sigma^{(n)}$ as obtained from Eq. (16). Outside this interval a destabilising negative damping coexists with a destabilising parametric resonance and, in our linearised model, the amplitudes grow exponentially without restriction.

For the symmetric system matrices as stated in Eq. (3), the upper sign in Eq. (15) corresponds to a parametric anti-resonance frequency while the lower sign corresponds to a classical parametric resonance frequency, as outlined in Ref. [13]. The opposite is the case if the parametric excitation matrices $\mathbf{Q}$, $\mathbf{P}$ would be skew-symmetric, see Refs. [21,27]. The stability boundary curves in Eq. (16) determine values of the parametric excitation frequency η for which vibration suppression can be achieved. These curves define a dense frequency interval of η within which damping by parametric excitation may occur. The strongest damping is achieved if the value of η is chosen at the centre η_0 of this interval. The analytical formula induces that the parametric anti-resonance frequency η_0 for the system in Fig. 1 is exactly equal to a parametric combination frequency $|\Omega_1 - \Omega_2|/n$. However, numerical calculations showed that the real stability boundary curve is shifted slightly from the analytical prediction [29]. Nevertheless, the width of the numerically obtained frequency interval is equal to the analytical one and analysing the analytical expressions is as meaningful as performing numerical analysis in order to optimise a desired system. An advantage of the analytical calculation is that the analytical expressions allow a direct optimisation while in case of a numerical analysis the shifted centre of the stable frequency interval has to be calculated separately for each value set of system parameters.

4. Optimisation

Previous investigations, e.g. Refs. [33,34], showed that it is advantageous to increase the interval of vibration suppression $\sigma^{(n)}$ for several reasons. First, an increased stability interval in Eq. (16) increases the robustness of the method, since fluctuations in the system parameters would have less influence on the performance. Secondly, a wider interval positively affects the transient behaviour during vibrations suppression. Two aspects in the optimisation of damping by stiffness excitation are considered: (a) maximising the robustness of the method with respect to changes of the frequency η and, (b) maximising the resulting amplification of system damping. Both criteria demand to maximise the stability interval. The constant parts of the system coefficients are considered to be fixed while the phase angles α_{12}, α_{02} and amplitude amplification factors ε_{01}, ε_{12}, ε_{02} determining the parametric excitations are optimised. A stiffness variation is considered to be optimal if it maximises the stability width for fixed n,

$$2\varepsilon\sigma^{(n)} \to \max \qquad \text{for} \qquad n = 1, 2, \ldots. \tag{18}$$

Since the stability interval $\sigma^{(n)}$ in Eq. (16) is inversely proportional to n in most cases only the leading Fourier coefficient a_1 is decisive.

Of practical importance is the case where one modal damping coefficient is negative:

$$\Theta_{11}\Theta_{22} < 0. \tag{19}$$

Here the conditions in Eq. (14) are no longer met and the negative damping is strong enough to destabilise the system without parametric excitation. For the system with parametric excitation the coefficient matrices in Eq. (3) are symmetric and, consequently, the parametric excitation term $Q_{12}Q_{21} + P_{12}P_{21}$ in Eq. (17) is always positive. Searching for a maximal suppression interval the stability conditions in Eq. (15) needs to be fulfilled. Inserting the second condition into Eq. (17) and restricting the optimisation to Eq. (19) implicates that $\sigma^{(n)}$ is always real. To maximise a real-valued $\sigma^{(n)}$ under the restrictions from above, the parametric excitation term needs to be maximised. A smooth quality function J is defined proportionally to the non-dimensional parametric excitation term that follows from Eqs. (8)–(10):

$$a_n^2(Q_{12}Q_{21} + P_{12}P_{21}) = \frac{2k_{01}^2 k_{12}^2}{(\Omega_1^2 - \Omega_2^2)^2 m_1^3 m_2} \ a_n^2 J(\alpha_{12}, \alpha_{02}, \varepsilon_{01}, \varepsilon_{12}, \varepsilon_{02}) \to \max, \tag{20}$$

which is a function of the phase angles and the amplitude amplification factors. The constant parts of the system coefficients are considered to be fixed so that Eq. (20) simplifies to

$$a_n^2 J(\alpha_{12}, \alpha_{02}, \varepsilon_{01}, \varepsilon_{12}, \varepsilon_{02}) \to \max. \tag{21}$$

Inserting the matrix entries from Eq. (3) into Eqs. (9) and (21) results in the quality function

$$J = -(1-a)\varepsilon_{01}\varepsilon_{12}\cos\alpha_{12} - a\varepsilon_{01}\varepsilon_{02}\cos\alpha_{02} + a(1-a)\varepsilon_{12}\varepsilon_{02}\cos(\alpha_{12} - \alpha_{02})$$
$$+ \tfrac{1}{2}\big(\varepsilon_{01}^2 + (1-a)^2\varepsilon_{12}^2 + a^2\varepsilon_{02}^2\big), \tag{22}$$

with the abbreviation

$$a = \frac{m_1 k_{02}}{m_2 k_{01}} = \left(\frac{\omega_2}{\omega_1}\right)^2, \tag{23}$$

where a defines a frequency ratio. The quality function J possesses the interesting property of being independent from the coupling stiffness k_{12} or any damping parameter. Note that Eq. (22) is a dimensionless energy-based quality function.

4.1. Optimal function shape

The method of suppressing vibrations of a negatively damped system has been studied extensively for the case of time-harmonic variations of the system parameters. In this section, the efficiency of different time-periodic, but not necessarily harmonic, variations are examined following Ref. [23]. Maximising the condition

in Eq. (21) for fixed phase angles and amplification factors demands maximising the Fourier coefficients $|a_n|$ and, consequently, adapting the shape function g of the stiffness variations in Eq. (2).

The largest value for the expression in Eq. (21) is found for a specific value n for which the Fourier coefficient is maximal,

$$|a_n| \rightarrow \max. \tag{24}$$

However, since the stability interval $\sigma^{(n)}$ in Eq. (16) is inversely proportional to n in most cases only the leading Fourier coefficient a_1 is decisive for the largest stability interval defined in Eqs. (18), (17). Fourier series and their leading coefficient for example shapes of g are listed in Table 1. The reference shape is the cosine function with a leading Fourier coefficient of one, $a_1 = 1$, as investigated in the main literature on damping by parametric excitation. According to Eq. (21), a harmonic stiffness excitation leads to an amplification factor a_1^2 of the quality function J equal to one. Applying a triangular excitation is equivalent to an amplification loss of 34% and for the case of a parabola shape the amplification is as less as 6%. An impulse-like or trapezoid shape function leads to a gain of up to 61% depending on the parameter φ. Consequently, the greatest enhancement, compared to a stiffness variation of the classical harmonic shape, is achieved for a simple rectangular shape for $n = 1$ and $\varphi = 0$, in which case

$$a_1 = \frac{4}{\pi} = 1.27. \tag{25}$$

For a system with two degrees of freedom with time-periodic stiffness parameters $k_{kl}(t)$ the optimal function is a simple rectangular shape, also known as an open-loop bang-bang control [35]. Counter-intuitively, impulse-like shapes, for which the fast dynamics of the signal are concentrated in a very small time interval, are not optimal. This extraordinary result means that a benefit of 61% can be achieved just by adjusting the shape of the stiffness variation function but without increasing the peak values $k_{kl}(1 \mp \varepsilon_{kl})$. This optimum is an analytical verification and generalisation of the extensive numerical studies performed for a bang-bang controller in Ref. [22] wherein only one stiffness parameter was varied periodically in time.

4.2. Optimal phase angles

In this section, optimal phase relations $\hat{\alpha}_{12}, \hat{\alpha}_{02}$ are derived for arbitrary amplitude amplification factors $\varepsilon_{01}, \varepsilon_{12}, \varepsilon_{02}$ and shape functions a_n. Since the argument of the cosine functions are linear in the parameters α_{12}, α_{02}, the quality function J is periodic with respect to these phase angles with a period of 2π and symmetric with respect to $0, \pi, 2\pi, \ldots$. Hence, all possible values of the quality function lie within the domain $[0, \pi] \times [0, \pi]$. Only positive amplification factors need to be considered because a negative factor is already accounted for by a phase angle of π. The first derivatives of J in Eq. (22) yield the conditions for extremal values [36]

$$\frac{\partial J}{\partial \alpha_{12}} = 0 : \quad (1 - a)\varepsilon_{12}(\varepsilon_{01} \sin \hat{\alpha}_{12} - a\varepsilon_{02} \sin(\hat{\alpha}_{12} - \hat{\alpha}_{02})) = 0, \tag{26a}$$

$$\frac{\partial J}{\partial \alpha_{02}} = 0 : \quad a\varepsilon_{02}(\varepsilon_{01} \sin \hat{\alpha}_{02} + (1 - a)\varepsilon_{12} \sin(\hat{\alpha}_{12} - \hat{\alpha}_{02})) = 0. \tag{26b}$$
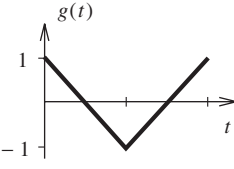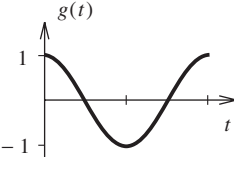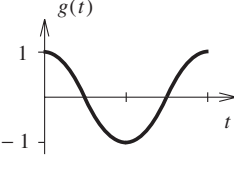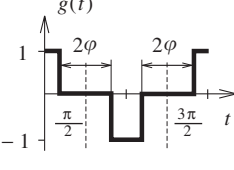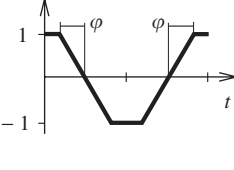
For $a, \varepsilon_{01}, \varepsilon_{12}, \varepsilon_{02} > 0, a \neq 0, 1$, the conditions above can be rewritten as

$$\sin(\hat{\alpha}_{12} - \hat{\alpha}_{02}) = \frac{1}{a} \frac{\varepsilon_{01}}{\varepsilon_{02}} \sin \hat{\alpha}_{12} = -\frac{1}{1 - a} \frac{\varepsilon_{01}}{\varepsilon_{12}} \sin \hat{\alpha}_{02}. \tag{27}$$

To decide whether the quality function is maximised the additional condition

$$\frac{\partial^2 J}{\partial(\alpha_{12}, \alpha_{02})} = a(1 - a)\varepsilon_{01}\varepsilon_{12}\varepsilon_{02}[-(1 - a)\varepsilon_{12} \cos \alpha_{12} \cos(\alpha_{12} - \alpha_{02})$$

$$-a\varepsilon_{02} \cos \alpha_{02} \cos(\alpha_{12} - \alpha_{02}) + \varepsilon_{01} \cos \alpha_{12} \cos \alpha_{02}] > 0 \tag{28}$$

Table 1
Fourier coefficients for different periodic function shapes

Shape	Fourier coefficients	Leading coefficient
Triangle	$a_m = \dfrac{1}{m^2}\dfrac{8}{\pi^2}$ $m = 2n-1,\ n = 1, 2, \ldots$	$a_1 = 0.81$
Cosine	$a_n = \begin{cases} 1, & n = 1 \\ 0, & n > 1 \end{cases}$ $n = 1, 2, \ldots$	$a_1 = 1$
Parabolah	$a_m = \dfrac{1}{m^3}\dfrac{32}{\pi^3}$ $m = 2n-1,\ n = 1, 2, \ldots$	$a_1 = 1.03$
Impulse-like	$a_m = \dfrac{\cos m\varphi}{m}\dfrac{4}{\pi}$ $m = 2n-1,\ n = 1, 2, \ldots$	$a_1 = 1.27 \cos \varphi$
Trapazoid	$a_m = \dfrac{\sin m\varphi}{m^2\varphi}\dfrac{4}{\pi}$ $m = 2n-1,\ n = 1, 2, \ldots$	$a_1 = 1.27\dfrac{\sin \varphi}{\varphi}$

has to be satisfied. For positive values of $\varepsilon_{01}, \varepsilon_{12}, \varepsilon_{02} \neq 0$, the following optimal phase angles $\hat{\alpha}_{kl}$ are found:

$$\hat{\alpha_{02}} = \pi \quad \text{and} \quad \hat{\alpha_{12}} = \begin{cases} \pi & \text{for } 0 < a < 1, \\ \text{any value} & \text{for } a = 1, \\ 0 & \text{for } a > 1. \end{cases} \tag{29}$$

The relation on the right hand side of Eq. (27) is similar to the famous Snell's law [36] that describes light or other waves passing through a boundary between two different isotropic media. However, contrary to light waves for which Hamilton's principle minimises an energy-related action, here the energy-related quality is maximised. The maximum value of the quality function in Eq. (22), the optimum, is derived by considering the

boundedness of the cosine functions in the interval $[-1, 1]$ and respecting $\varepsilon_{01}, \varepsilon_{12}, \varepsilon_{02} \geqslant 0$ and $a > 0$

$$\max\{J\} = |1 - a|\varepsilon_{01}\varepsilon_{12} + a\varepsilon_{01}\varepsilon_{02} + a|1 - a|\varepsilon_{12}\varepsilon_{02} + \tfrac{1}{2}(\varepsilon_{01}^2 + (1 - a)^2\varepsilon_{12}^2 + a^2\varepsilon_{02}^2)$$
$$= \tfrac{1}{2}(\varepsilon_{01} + \varepsilon_{12}|1 - a| + a\varepsilon_{02})^2. \tag{30}$$

Figs. 3 and 4 show the quality function J as a function of the relative phase angles α_{12}, α_{02} for fixed amplitude amplification factors $\varepsilon_{01}, \varepsilon_{12}, \varepsilon_{02}$. The value ranges for the phase angles are normalised to the interval $[0, 1]$. The symmetry of the quality function with respect to 0 and π leads to horizontal tangential planes at the domain borders. The variation of the amplitude amplification factors ε_{kl} in the particular sub-figure respects the constraint $\varepsilon_{01} + \varepsilon_{12} + \varepsilon_{02} = 0.6 = \text{const.}$ The amplification factor ε_{01} is chosen to be the reference excitation and is fixed. Varying these amplification factors, while respecting the constraint condition above, deforms the resulting shape of the quality function.

Typical shapes of the quality function J for small frequency ratio, $a < 1$, are plotted in Fig. 3. For non-vanishing amplification factors ε_{kl} the optimal phase angles for the maximum value are found at the position $(\alpha_{12}, \alpha_{02}) = (\pi, \pi)$, as derived analytically in Eq. (29), see Figs. 3b and c. If one of the amplification factors ε_{12}, ε_{02} vanishes then the quality function J becomes independent of the corresponding phase angle α_{12}, α_{02} and the resulting shape degenerates, see Fig. 3a or d. In both cases the position (π, π) remains optimal. Performing the linear adaptation of the amplification factors $\varepsilon_{01}, \varepsilon_{12}, \varepsilon_{02}$ respecting the mentioned constraint reveals that the shape of the quality function J is transformed from one degenerated shape in Fig. 3a, through the general shapes in Figs. 3b and c, into the degenerated shape in Fig. 3d. The typical shapes of the quality function J for large frequency ratio, $a = 4 > 1$, are plotted in Fig. 4. In this case, similar function shapes of the quality function J as in the case of $a < 1$ are obtained but now the optimal phase angles are located at $(\pi, 0)$ for general nonzero amplification factors $\varepsilon_{12}, \varepsilon_{02}$, according to Eq. (29). Note that for non-vanishing amplification factors ε_{kl} the optimal phase angles for the maximum value are found at the position $(0, \pi)$ or (π, π), as derived analytically in Eq. (29). Beside this optimal position the remaining three corner positions of $(0, 0)$, $(0, \pi)$, $(\pi, 0)$ and (π, π) represent extremal positions, of which some of them are suboptimal.
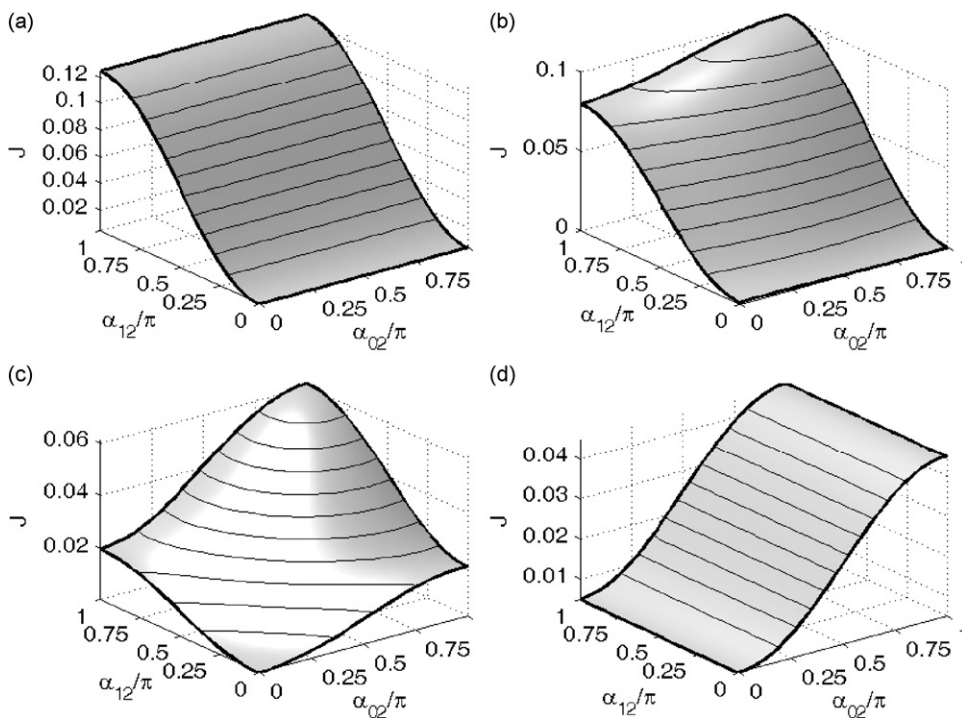

Fig. 3. Quality function for $a = 0.25 (< 1)$ as a function of the phase angles α_{kl} at $\varepsilon_{01} = 0.2$ and different values of amplification factors ε_{12}, ε_{02}: (a) $\varepsilon_{12} = 0.4$, $\varepsilon_{02} = 0$, (b) $\varepsilon_{12} = 0.3$, $\varepsilon_{02} = 0.1$, (c) $\varepsilon_{12} = 0.1$, $\varepsilon_{02} = 0.3$, and (d) $\varepsilon_{12} = 0$, $\varepsilon_{02} = 0.4$.
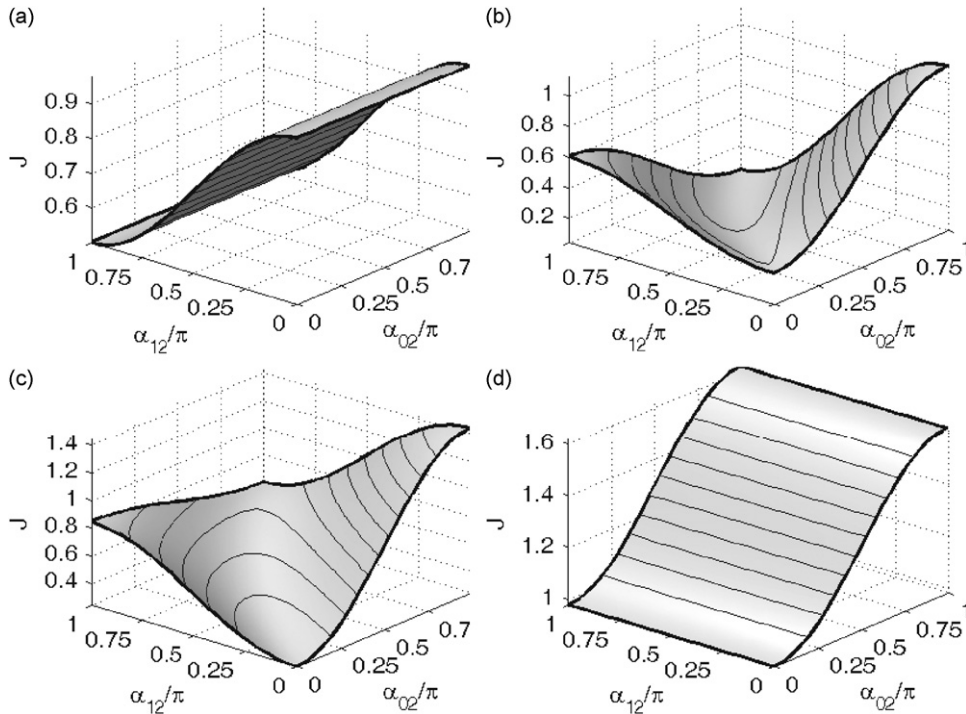
Fig. 4. Same as Fig. 3 but for $a = 4 (> 1)$.

The special value $a = 1$ represents a symmetric arrangement with respect to eigenfrequencies that arise if the natural frequency of each subsystem coincide, $\omega_1 = \sqrt{k_1/m_1} = \sqrt{k_2/m_2} = \omega_2$, compare to Fig. 1. Due to the previous results, the optimal value of the quality function is found at least at the phase angles $(0, \pi)$ and (π, π). Evaluating the quality function defined in Eq. (22) at this critical value of a we obtain

$$J|_{a=1} = \tfrac{1}{2}(\varepsilon_{01}^2 + \varepsilon_{02}^2) - \varepsilon_{01}\varepsilon_{02}\cos\alpha_{02}. \tag{31}$$

The quality function loses its dependency on ε_{12} as well as on α_{12}. Due to the symmetry of J in the variables $\varepsilon_{01}, \varepsilon_{02}$, a variation of ε_{01} is equivalent to a variation of ε_{02}. For fixed amplification factors ε_{kl} the resulting function shape of J simplifies to the shapes similar to Fig. 3d or 4d, since the special cases $a = 1$ and $\varepsilon_{12} = 0$ coincide, see Eq. (29). For the critical frequency ratio $a = 1$ the optimal function value of J is found at the phase angle $\alpha_{02} = \pi$ and arbitrary phase angle α_{12}.

For the very special case where all amplification factors are equal, $\varepsilon_{01} = \varepsilon_{12} = \varepsilon_{02} = \varepsilon$, the expression for the quality function in Eq. (21) simplifies and the solutions derived in Eq. (29) yield

$$J(0, \pi, \varepsilon, \varepsilon, \varepsilon) = 2a^2\varepsilon^2 \quad \text{and} \quad J(\pi, \pi, \varepsilon, \varepsilon, \varepsilon) = 2\varepsilon^2. \tag{32}$$

Consequently, the optimal value of J at the global maximum depends on a at high frequency ratios, $a > 1$, while the global maximum remains constant at low frequency ratios, $a \leqslant 1$. The optimal distribution of the amplification factors is investigated in the following paragraph.

4.3. Optimal amplification factors

In a real device for parametric excitation the power supply, in general, is limited by a mechanical or electrical load, as the maximum force or the maximum current. In this section we are searching for an optimal distribution of the amplification factors $\varepsilon_{01}, \varepsilon_{12}, \varepsilon_{02}$ under the constraint condition that the maximum value of the potential energy is restricted

$$h(\varepsilon_{01}, \varepsilon_{12}, \varepsilon_{02}) = \varepsilon_{01}k_{01} + \varepsilon_{12}k_{12} + \varepsilon_{02}k_{02} \leqslant C \tag{33}$$

and $\varepsilon_{01}, \varepsilon_{12}, \varepsilon_{02} \geq 0$, following Ref. [25]. Since the constraint condition in Eq. (33) does not depend on the phase angles α_{12}, α_{02}, the optimisation of the phase angles and the amplification factors are decoupled and the phase angles derived in Eq. (26b) remains optimal. According to the definition in Eq. (22) and respecting the optimal phase angles found in Eq. (29), the quantity $J(\hat{\alpha}_{12}, \hat{\alpha}_{02}, \varepsilon_{01}, \varepsilon_{12}, \varepsilon_{02})$ is strictly monotonically increasing with increasing amplification factors ε_{kl},

$$\frac{\partial J}{\partial \varepsilon_{01}} = \varepsilon_{01} + |1 - a|\varepsilon_{12} + a\varepsilon_{02} > 0, \quad \frac{\partial J}{\partial \varepsilon_{12}} = |1 - a|\frac{\partial J}{\partial \varepsilon_{01}} > 0, \quad \frac{\partial J}{\partial \varepsilon_{02}} = a\frac{\partial J}{\partial \varepsilon_{01}} > 0. \tag{34}$$

The function h represents a plane which is monotonically increasing in terms of the amplification factors because the stiffness parameters k_{kl} possess in physical meaningful systems only positive values ($\partial h/\partial k_{kl} = k_{kl} > 0$). Consequently, a multi-variable optimisation using the method of Lagrange multipliers cannot be applied and the optimum values are located without exception at the boundary of the parameter domain resulting from the constraint h.

At the optimal positions found in Eq. (29) for $a > 0$, the quality function $J(\varepsilon_{01}, \varepsilon_{12}, \varepsilon_{02}, \alpha_{12}, \alpha_{02})$ simplifies to $J(\varepsilon_{01}, \varepsilon_{12}, \varepsilon_{02})$ satisfying Eq. (30). The constraint condition in Eq. (33) represents a plane in the parameter domain $\varepsilon_{01}, \varepsilon_{12}, \varepsilon_{02}$, which is positioned by using the constant potential C. Since J is strictly monotonically increasing for increasing amplification factors, the optimum lies on the triangle span by $h = C$ and $\varepsilon_{kl} \geq 0$. Substituting one parameter, e.g. ε_{12}, by using the constraint condition in Eq. (33) for positive stiffness parameters k_{01}, k_{12}, k_{02}, and consequently positive system potential C, results in the mapping

$$J(\varepsilon_{01}, \varepsilon_{12}, \varepsilon_{02}) \mapsto \hat{J}(\varepsilon_{01}, \varepsilon_{02}) = \frac{1}{2}\left(\varepsilon_{01} + \frac{C - \varepsilon_{01}k_{01} - \varepsilon_{02}k_{02}}{k_{12}}|1 - a| + a\varepsilon_{02}\right)^2. \tag{35}$$

Respecting the constraint condition limits the intervals of ε_{kl} for fixed positive value of C to $[0, C/k_{kl}]$. To find the global maximum of the quality function J only the values of the mapped function $\hat{J}$ at the three parameter combinations $\hat{J}(\max(\varepsilon_{01}), 0)$, $\hat{J}(0, \max(\varepsilon_{02}))$ and $\hat{J}(0, 0)$ need to be compared. Note that the expression $\hat{J}(0, 0)$ is equivalent to $J(0, \max(\varepsilon_{12}), 0)$. The optimal amplitude amplification factors at the phase angles Eq. (29) are found to be one of the following sets of amplification factors:

$$(\mathbf{e}_1, \mathbf{e}_2, \mathbf{e}_3) = \{(\varepsilon_{01\max}, \quad 0, \quad 0), (0, \quad \varepsilon_{12\max}, \quad 0), (0, \quad 0, \quad \varepsilon_{02\max})\}, \tag{36}$$

with the abbreviations $\mathbf{e}_i = (\varepsilon_{01}, \varepsilon_{12}, \varepsilon_{02})$ and $\varepsilon_{kl\max} = \max(\varepsilon_{kl}) = C/k_{kl}$. From previous studies [13,33,20] it is known that, for the systems considered so far, higher amplitudes lead to an increased stability interval in Eqs. (16), (17). The sets in Eq. (36) prove this dependency in general.

Comparing the values of J at the sets in Eq. (36) decides which of these parameter combinations is optimal. Introducing the following set of characteristic parameters

$$R_{12} = \frac{k_{12}}{k_{01}}, \quad R_{02} = \frac{k_{02}}{k_{01}}, \quad M = \frac{m_1}{m_2}, \tag{37}$$

where $MR_{02} = a$, the decisive conditions can be written compactly as

$$J(\mathbf{e}_1) \gtreqless J(\mathbf{e}_3): \quad M \lesseqgtr 1, \tag{38a}$$

$$J(\mathbf{e}_3) \gtreqless J(\mathbf{e}_2): \quad \frac{MR_{12}}{|1 - a|} = \frac{MR_{12}}{|1 - MR_{02}|} \gtreqless 1, \tag{38b}$$

$$J(\mathbf{e}_1) \gtreqless J(\mathbf{e}_2): \quad \frac{R_{12}}{|1 - a|} = \frac{R_{12}}{|1 - MR_{02}|} \gtreqless 1. \tag{38c}$$

It is quite remarkable that the position of the global maximum at the boundary is determined by only three parameters, namely M, R_{12} and R_{02} in Eq. (37). The achievable maximum value of the quality function is determined by

$$J_{opt} = \frac{1}{2}(\max\{\varepsilon_{01\,\max}, |1 - a|\varepsilon_{12\,\max}, a\varepsilon_{02\,\max}\})^2. \tag{39}$$

Note that the optimal parameter set is independent of any damping parameter, as is the quality function in Eq. (22) itself. Consequently, whether the negative damping is located parallel to the stiffness that is

periodically varied or not does not influence the optimal parameter set at all. Furthermore, for $\varepsilon_{12} = 0$ the optimal parametric excitation is situated at the smaller mass according to the condition in Eq. (38a) and is independent of the stiffness ratios R_{12} and R_{02}.

Sometimes only the simplified system with $k_{02} = 0$ is considered, see Fig. 1. For vanishing stiffness parameter k_{02} the amplification factor ε_{02} does not exist, $\varepsilon_{02} = 0$, and in Eq. (38) only the last condition is relevant

$$R_{12} = \frac{k_{12}}{k_{01}} \gtrless 1 \quad \text{for } J(\mathbf{e}_1) \gtrless J(\mathbf{e}_2). \tag{40}$$

In the special case for which all stiffness parameters are equal, $k_{01} = k_{12} = k_{02} = k$, an assumption also made for the numerical studies performed in Ref. [24], the characteristic parameters simplify to $R_{12} = R_{02} = 1$ and $a = M$. Here, the parameter set $\mathbf{e}_2$ can only be suboptimal and the conditions in Eq. (38) simplify to the single condition in Eq. (38a).

4.4. Summary

In the previous sections, a system with multiple non-harmonic stiffness variations was considered for which conditions for an optimal configuration were derived analytically by maximising the stability width in Eq. (18) and, consequently, the weighted quality function in Eq. (21). These conditions reveal how the maximum gain in stability depends on the amplitude, the phase and the shape function of the periodic stiffness excitation. Only four characteristic parameters determine the globally optimal stiffness variation: the maximum Fourier coefficient a_n in Eq. (24), and the three parameters M, R_{12}, R_{02} introduced in Eq. (37). The frequency ratio introduced in Eq. (23) can be rewritten as $a = MR_{02}$.

The objective in Eq. (21) can be met by maximising a specific Fourier coefficient a_n in Eq. (24) which is, in general, the leading coefficient a_1. For a bounded stiffness variation, the optimum shape is found to be a rectangle for which the weighting factor in Eq. (21) is increased for $n = 1$ by 61% according to Eq. (25). Optimal phase angles α_{12}, α_{02} and amplification factors ε_{01}, ε_{12}, ε_{02} for the stiffness variations introduced in Eq. (2) are found by maximising the quality function in Eq. (22). A single characteristic parameter suffices to state the optimum configuration for the phase angles in Eq. (29). This condition is independent of the coupling stiffness k_{12}. Optimal amplification factors are derived for a constraint in the potential energy Eq. (33) that leads to the three conditions in Eq. (38) using the definitions in Eqs. (36) and (37).

5. Numerical example

In order to examine the analytical results obtained for vibration suppression the dynamic stability of a specific system is compared at different phase angles and a harmonic stiffness excitation as well as the most favourable rectangular excitation. For the numerical study the configuration $k_{02} = 0, c_{02}, \varepsilon_{02} = 0$, in Fig. 1 and Eq. (2) is examined, which is a system similar to the one investigated in Refs. [13,33] but with an additional stiffness excitation of k_{12}. Two stiffness coefficients are varied periodically, k_{01} and k_{12}, with a phase relation α_{12} and amplification factors $\varepsilon_{01} = \varepsilon_{12} = \varepsilon$. A flow-induced self-excitation force is assumed to be acting on the second mass and is modelled by a linearised van der Pol model,

$$F_{\text{SE}} = (c_1 - c_0 U^2)\dot{x}_2, \tag{41}$$

where U is the velocity of a steady wind flow and c_1, c_0 are geometric constants [15]. If the flow velocity U is sufficiently high the overall damping coefficient becomes negative in which case the self-excitation is destabilising. The following non-dimensional parameter set is used, see Ref. [33] for more details,

$$\frac{m_1}{m_2} = 5, \quad \frac{c_1 - c_0 U^2}{m_1 \omega_1} = -0.01, \quad \frac{c_2}{m_2 \omega_1} = 0.14, \quad \varepsilon = 0.25 \quad \text{and} \quad \alpha_{12} \tag{42}$$

with $\omega_1 = \sqrt{k_{01}/m_1}$ and $\omega_2 = \sqrt{k_{12}/m_2}$. For a certain physical system specific values for some of the dimensional parameters have to be chosen additionally. These conditions satisfy the first condition in

Eqs. (15), (16) and additionally Eq. (19), so that the system without parametric excitation, $\varepsilon = 0$, is dynamically unstable due to negative damping.

Stability maps for a system with harmonic stiffness excitation are shown in Fig. 5, derived by direct numerical integration for fixed system parameters of each sample system, see Ref. [37]. Stability is indicated by a shaded region. For our specific system the dimensionless parameter a introduced in Eq. (23) vanishes and the optimal phase angle is found in Eq. (29), $\hat{\alpha}_{12} = 180°$. The influence of varying the phase angle α_{12} from $0°$ towards its optimum value $180°$ is shown in Fig. 5. If both stiffness excitations at k_{01} and k_{12} are performed synchronously, $\alpha_{12} = 0°$, then the amplification factor ε in Eq. (42) is too small to satisfy the stability condition in Eq. (15) and damping by parametric excitation is not possible. Increasing the phase relation first enables and thereafter even increases the effect of damping by parametric excitation near the parametric anti-resonance frequency in Eq. (1). Furthermore, even the destabilising character of the classical parametric resonance frequency $2\Omega_2$ is reduced the closer α_{12} becomes to $\hat{\alpha}_{12}$. As predicted by the analytical analysis, the maximum stability region for damping by parametric excitation is obtained at $\hat{\alpha}_{12}$ in Fig. 5d.

The effect of a rectangular shape function on the stability regions is presented in Fig. 6 for a phase angle of $120°$ and the optimum value $\hat{\alpha}_{12}$. Compared to the corresponding harmonic shape function in Figs. 5c and d, the anti-resonant stability region is widened. For our specific system the anti-resonance region at optimum phase angle but harmonic shape function in Fig. 5d is equivalent to a rectangular stiffness excitation at $120°$ in
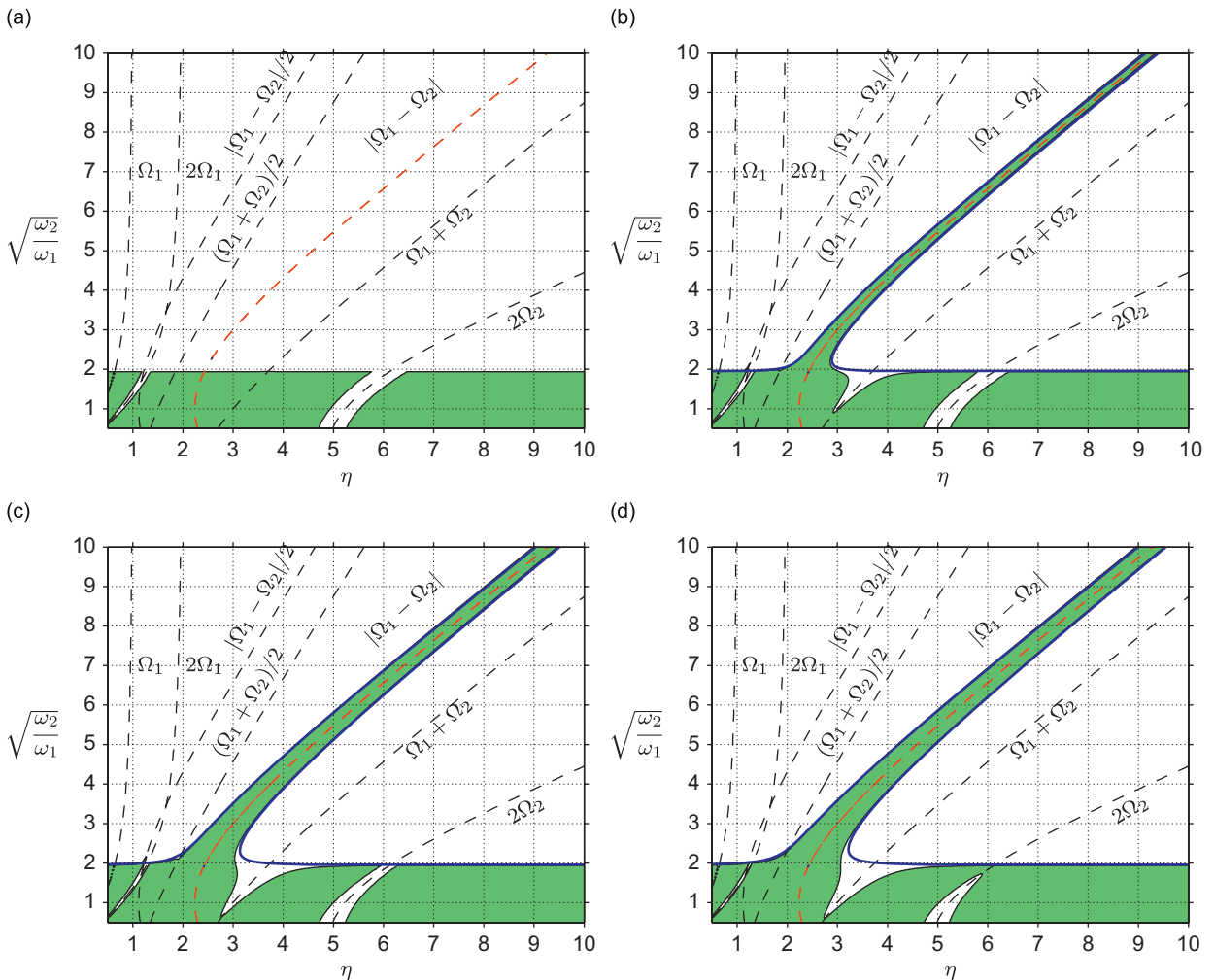

Fig. 5. Stability maps for different values of phase angle α_{12} at harmonic stiffness excitation: (a) $\alpha_{12} = 0°$, (b) $\alpha_{12} = 60°$, (c) $\alpha_{12} = 120°$, and (d) $\alpha_{12} = 180° = \hat{\alpha}_{12}$.
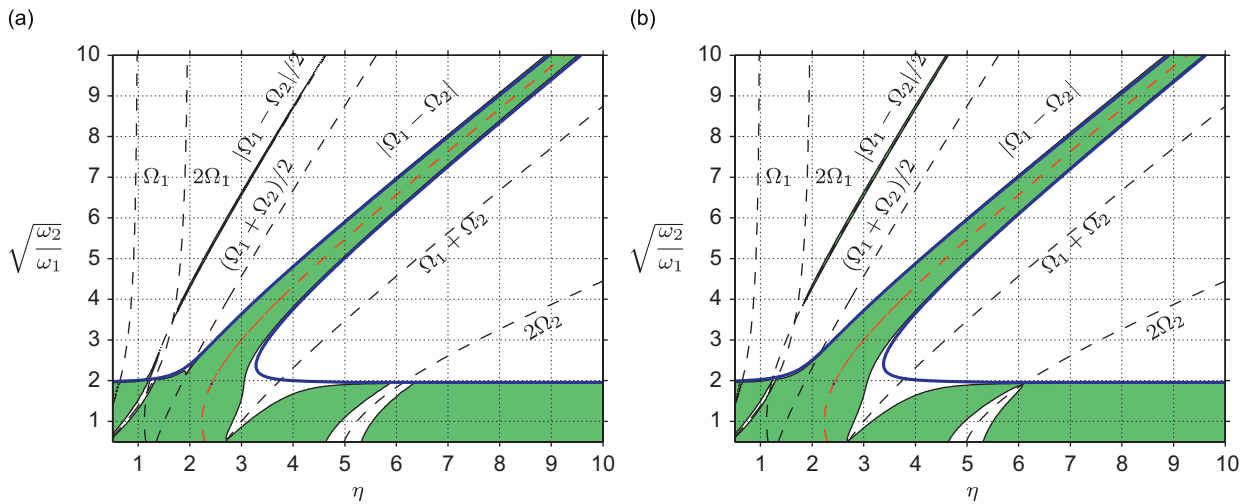
Fig. 6. Stability maps for rectangular shape function: (a) $\alpha_{12} = 120°$ and (b) $\alpha_{12} = 180° = \hat{\alpha}_{12}$.
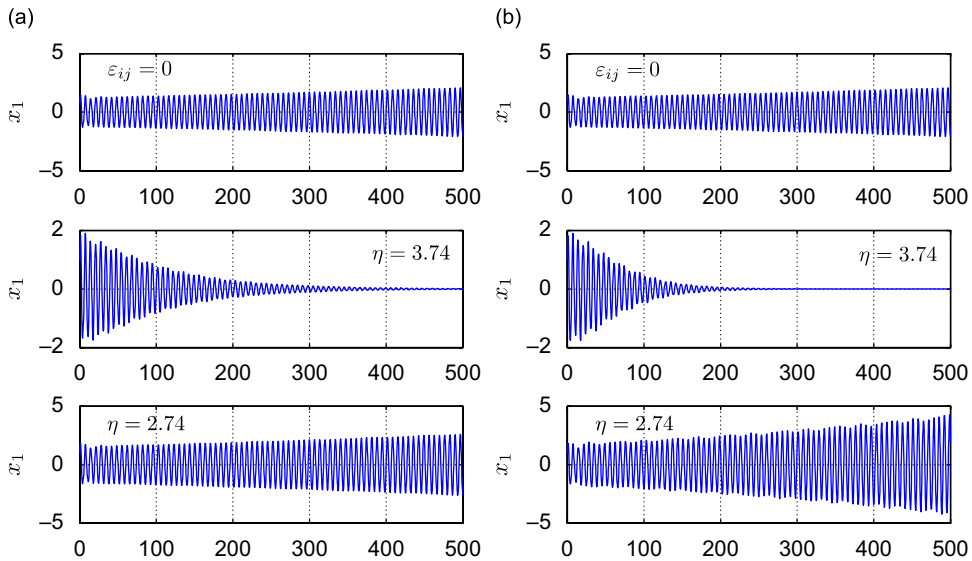

Fig. 7. Time histories at $Q = 4.0$ for different function shapes of stiffness excitation: (a) cosine stiffness excitation and (b) rectangular stiffness excitation.

Fig. 6. The largest stability region near $|\Omega_1 - \Omega_2|$ is obtained for a rectangular shape function and optimal phase angle of 180°. Note that the effective amplification factor $a_1\varepsilon$ becomes so large that even an anti-resonance region near the frequency $|\Omega_1 - \Omega_2|/2$ can be examined. Comparing Figs. 5c and d with Fig. 7 reveals that not only the stability regions are enlarged but the instability regions as well.

Finally, time series of the vibration amplitude x_1 for a harmonic and a rectangular stiffness excitation at two different parametric excitation frequencies are compared in Figs. 7a and b. The vibration amplitudes of x_2 are qualitatively similar and are therefore omitted. The positive effect of damping by parametric excitation on the transient behaviour using different shape functions is highlighted. Near the parametric anti-resonance frequency η_0 in Eq. (1), the centre of the frequency interval in Eq. (16), the vibrations are suppressed most efficiently. With increasing distance of η from η_0 the vibrations are suppressed less effectively and amplitudes decay slower. At $\eta = \eta_0 + \varepsilon\sigma$ the stability boundary is reached and the suppression interval ends. If the excitation frequency η is equal to the parametric anti-resonance frequency $\eta_0^{(1)} = |\Omega_1 - \Omega_2| = 3.74$ the

vibration can be successfully suppressed. Note that a frequency of $\eta = 2.74$ outside the suppression interval and close to the resonance frequency Ω_1 results in increasing vibrations due to the destabilising self-excitation. The comparison of the time histories confirms the analytical predictions that the vibrations are suppressed faster using a rectangularly shaped stiffness variation.

6. Conclusions

A general linear two-mass is investigated which is unstable due to negative damping and is stabilised by the interaction with multiple parametric stiffness excitations. From previous studies it is known that a harmonic variation of a single stiffness coefficient can stabilise an otherwise unstable system. In this paper, a system with multiple non-harmonic stiffness variations is considered. Analytical conditions are derived for an optimal configuration to achieve the largest frequency interval for vibration suppression. These conditions found confirm and generalise former numerical results for a single set of parameters and show how the maximum gain in stability depends on the amplitude, the phase, the location and the shape function of the periodic stiffness excitation.

The effectiveness of different periodic shape functions is compared to a rectangular shape function which turns out to be the most favourable variation since it maximises the leading Fourier coefficient. The optimal rectangular shape results in a gain of the suppression interval width of 61% compared to a harmonic stiffness variation. Thereby it is possible to increase the suppression interval only by adjusting the shape, while the minimum and maximum values of the stiffness variation remain unchanged. The optimal distribution of the phase angles between multiple stiffness variations depends solely on the frequency ratio of two single-mass subsystems. Only three conditions are decisive for the optimal distribution of the amplitudes of a multiple stiffness variation under a constraint in the potential energy. These analytical predictions are verified by a numerical stability analysis of an example system. With the help of the criteria obtained, we are capable of optimising a system with general time-harmonic variation of one or more stiffness coefficients with constraint in potential energy.

References

[1] T. Yamamoto, Y. Ishida, *Linear and Nonlinear Rotordynamics*, Wiley, New York, 2001.
[2] M.A. Santos Neves, N. Perez, O. Lorca, Analysis of roll motion and stability of a fishing vessel in head seas, *Ocean Engineering* 30 (2003) 921–935.
[3] H.N. Ozguven, D.R. Houser, Mathematical models used in gear dynamics—a review, *Journal of Sound and Vibration* 121 (1988) 383–411.
[4] V.V. Bolotin, *Dynamic Stability of Elastic Systems*, Holden-Day, San Francisco, 1964.
[5] V.A. Yakubovich, V.M. Starzhinskii, *Linear Differential Equations with Periodic Coefficients* (two volumes), Wiley, London, 1975.
[6] T. Yamamoto, A. Saito, On the vibrations of summed and differential types under parametric excitation, *Memoirs of the Faculty of Engineering* 22 (1) (1970) 54–123.
[7] R. Mickens, *An Introduction to Nonlinear Oscillations*, Cambridge University Press, Cambridge, 1981.
[8] K. Klotter, *Technische Schwingungslehre*, Springer, Berlin, 1988 [in German].
[9] M. Cartmell, *Introduction to Linear, Parametric and Nonlinear Vibrations*, Chapman & Hall, London, 1990.
[10] A. Seyranian and A. Mailybaev, Multiparameter Stability Theory with Mechanical Applications, Stability, Vibration and Control of Systems, Vol. 13, World Scientific, Singapore, 2003.
[11] J.J. Thomsen, *Vibrations and Stability—Advanced Theory, Analysis and Tools*, second ed., Springer, Berlin Heidelberg, New York, 2003.
[12] W.-C. Xie, *Dynamic Stability of Structures*, Cambridge University Press, Cambridge, 2006.
[13] A. Tondl, To the problem of quenching self-excited vibrations, *Acta Technica CSAV* 43 (1998) 109–116.
[14] J.P. Den Hartog, *Mechanical Vibrations*, Dover, New York, 1984.
[15] R.D. Blevins, *Flow-Induced Vibration*, second ed., Van Nostrand Reinhold, New York, 1990.
[16] A. Tondl, *Quenching of Self-Excited Vibrations*, Academy of Sciences, Czech Republic, 1991.
[17] A. Tondl, The method for determination of instability of quasiharmonic vibrations, *Aplikace matematiky* 4 (1959) 278–289 [in Czech].
[18] S. Fatimah, F. Verhulst, Suppressing flow-induced vibrations by parametric excitation, *Nonlinear Dynamics* 23 (2003) 275–297.
[19] Abadi, Nonlinear Dynamics of Self-Excitation in Autoparametric Systems, PhD Thesis, Utrecht University, 2003.
[20] F. Dohnal, Damping of Mechanical Vibrations by Parametric Excitation, PhD Thesis, Vienna University of Technology, 2005.
[21] F. Dohnal, Damping by parametric stiffness excitation—resonance and anti-resonance, *Journal of Vibration and Control* 14 (2008) 669–688.

[22] K. Makihara, H. Ecker, F. Dohnal, Stability analysis of open-loop stiffness control to suppress self-excited vibrations, *Journal of Vibration and Control* 11 (2005) 643–669.

[23] F. Dohnal, Suppression of self-excited vibrations by non-smooth parametric excitation, in: I. Dobiáš (Ed.), *Proceeding of the Dynamics of Machines*, Prague, Czech Republic, February 2004, pp. 27–34.

[24] H. Ecker, Optimal phase relationship for a system with multi-location parametric excitation, in: L. Pesek (Ed.), *Proceeding of the Dynamics of Machines*, Prague, Czech Republic, February 2005, pp. 31–38.

[25] F. Dohnal, Optimal multi-location harmonic stiffness excitation, in: L. Pesek (Ed.), *Proceeding of the Dynamics of Machines*, Prague, Czech Republic, February 2007, pp. 35–42.

[26] N. Eicher, *Einführung in die Berechnung parametererregter Schwingungen*, Technical University of Berlin, TUB-Documentation, 1981 [in German].

[27] F. Dohnal, General parametric stiffness excitation—anti-resonance frequency and symmetry, *Acta Mechanica* 196 (2008) 15–33.

[28] F. Verhulst, Nonlinear Differential Equations and Dynamical Systems. Texts in Applied Mathematics, Vol. 50 Springer-Verlag, Berlin Heidelberg, New York, 2000.

[29] F. Dohnal, F. Verhulst, Averaging in vibration suppression by parametric stiffness excitation, *Nonlinear Dynamics* 54 (2008) 231–248.

[30] A.H. Nayfeh, D.T. Mook, *Nonlinear Oscillations*, third ed., Wiley, New York, 1995.

[31] H. Bilharz, Bemerkung zu einem Satze von Hurwitz, *Zeitschrift für angewandte Mathematik und Mechanik (ZAMM), Applied Mathematics and Mechanics* 24 (2) (1944) 77–82 [in German].

[32] F. Gantmacher, Matrizenrechnung Teil II, spezielle Fragen und Anwendungen, Hochschulbücher für Mathematik, VEB Deutscher Verlag der Wissenschaften, Berlin, 1966 [in German].

[33] A. Tondl, H. Ecker, Cancelling of self-excited vibrations by means of parametric excitation, *Proceeding of the ASME Design Engineering Technical Conference (DETC)*, Las Vegas, Nevada, September 1999.

[34] F. Dohnal, H. Ecker, A. Tondl, Vibration control of self-excited oscillations by parametric stiffness excitation, *Proceedings of the Eleventh International Congress of Sound and Vibration (ICSV11)*, St. Petersburg, 2004, pp. 339–346.

[35] L. Sonneborn, F. Van Vleck, The bang–bang principle for linear control systems, *SIAM Journal Control* 2 (1965) 151–159.

[36] P.A. Tipler, R. Llewellyb, *Modern Physics*, third ed., W.H. Freeman, New York, 2003.

[37] W.T. Wu, J.H. Griffin, J.A. Wickert, Perturbation method for the Floquet eigenvalues and stability boundary of periodic linear systems, *Journal of Sound and Vibration* 182 (2) (1995) 245–257.